Applied Physics Letters

Absolute dual-comb spectroscopy at 1.55 μm by free-running Er:fiber lasers

Cite as: Appl. Phys. Lett. **104**, 231102 (2014); https://doi.org/10.1063/1.4882862
Submitted: 01 April 2014 . Accepted: 29 May 2014 . Published Online: 09 June 2014

Marco Cassinerio, Alessio Gambetta, Nicola Coluccelli, Paolo Laporta, and Gianluca Galzerano

View Online Export Citation CrossMark

ARTICLES YOU MAY BE INTERESTED IN

Real-time dual-comb spectroscopy with a free-running bidirectionally mode-locked fiber laser
Applied Physics Letters **108**, 231104 (2016); https://doi.org/10.1063/1.4953400

Invited Article: A compact optically coherent fiber frequency comb
Review of Scientific Instruments **86**, 081301 (2015); https://doi.org/10.1063/1.4928163

Development of ultrafast time-resolved dual-comb spectroscopy
APL Photonics **2**, 041301 (2017); https://doi.org/10.1063/1.4976730

© 2014 AIP Publishing LLC.

Absolute dual-comb spectroscopy at 1.55 μm by free-running Er:fiber lasers

Marco Cassinerio, Alessio Gambetta,[a] Nicola Coluccelli, Paolo Laporta, and Gianluca Galzerano
Istituto di Fotonica e Nanotecnologie - CNR and Dipartimento di Fisica del Politecnico di Milano, Piazza L. Da Vinci 32, 20133 Milano, Italy

(Received 1 April 2014; accepted 29 May 2014; published online 9 June 2014)

We report on a compact scheme for absolute referencing and coherent averaging for dual-comb based spectrometers, exploiting a single continuous-wave (CW) laser in a transfer oscillator configuration. The same CW laser is used for both absolute calibration of the optical frequency axis and the generation of a correction signal which is used for a real-time jitter compensation in a fully electrical feed-forward scheme. The technique is applied to a near-infrared spectrometer based on a pair of free-running mode-locked Er:fiber lasers, allowing to perform real-time absolute-frequency measurements over an optical bandwidth of more than 25 nm, with coherent interferogram averaging over 1-s acquisition time, leading to a signal-to-noise ratio improvement of 29 dB over the 50 μs single shot acquisition. Using 10-cm single pass cell, a value of 1.9×10^{-4} cm^{-1} Hz$^{-0.5}$ noise-equivalent-absorption over 1 s integration time is obtained, which can be further scaled down with a multi-pass or resonant cavity. The adoption of a single CW laser, together with the absence of optical locks, and the full-fiber design makes this spectrometer a robust and compact system to be employed in gas-sensing applications. © *2014 AIP Publishing LLC*.
[http://dx.doi.org/10.1063/1.4882862]

Optical frequency combs (OFCs)[1,2] have become a common tool in frequency metrology and high resolution spectroscopy laboratories. Their capability of down-linking the domain of optical frequencies to that of radiofrequency (RF) standards has paved the way for optical frequency measurements with an absolute reference for the optical frequencies axis.[3] The possibility of broadband parallel detection has also made OFCs very appealing for building new classes of spectrometers operating with an unprecedented mix of sensitivity, acquisition speed, resolution, and accuracy for trace detection of molecular compounds of interest in medicine (bio-markers in exhaled breath), environment (pollutants, greenhouse gases), and security (hazardous gases, explosive vapors).[4–10] Since its first implementation[11,12] the dual-comb spectroscopy technique has proven to be a powerful method for real time detection of multiple molecular gas compounds and has been successfully applied to different spectral regions, ranging from visible to far-infrared (IR).[9–15] In a frequency domain picture, the principle of operation is the following: a first comb with pulse repetition frequency f_r passes through the gas sample and recombines onto a fast photodetector (PD) together with a second comb with slightly detuned repetition frequency $f_r + \Delta f_r$. The second comb acts as a local oscillator, heterodyning the optical spectrum of the first comb to an RF replica with frequency axis downscaled by the ratio $\Delta f_r/f_r$. In the time domain, an interferogram is recorded at the output of the detector, analogously to a Fourier Transform InfraRed (FTIR) spectrometer. The interferogram trace recorded in a dual-comb setup is a periodic waveform with a repetition period of $\Delta T_r = \Delta f_r^{-1}$ which usually ranges from tens of μs to few ms. Thanks to the very short acquisition times and the coherence properties of the comb that allow the injection in a multi-pass cell or a high finesse cavity filled with the gas sample,[10] very low levels of noise-equivalent-absorption (NEA) at 1 s averaging can be reached for the single shot acquisition, of the order of $\sim 10^{-10}$ cm^{-1} Hz$^{-0.5}$. To further reduce the minimum detectable absorption coefficient $\alpha_{min} = \mathrm{NEA}/\sqrt{T}$, the integration time can be increased by coherently accumulating an high number of subsequent interferograms. In order to do so, the relative coherence time between the two combs must exceed the acquisition time or, in other words, the timing jitter between the two combs has to be reduced to a fraction of the optical carrier period $T_r = 1/f_r$. Different approaches have been pursued in literature to reach this goal. A first approach, adopted by Coddington *et al.*,[9] is to fully stabilize both combs against a pair of ultra-stable continuous-wave (CW) lasers which are also used for absolute optical referencing. Alternatively, it is possible to exploit an optical reference to detect the comb jitter and adaptively compensate each interferogram, as done by Ideguchi *et al.*[16] This latter setup is simpler, because does not involve optical phase-locked loops, and its more suited in practical applications, since it does not require the use of high-finesse cavities neither particular arrangements to isolate the system from environment. An intermediate scheme, adopted by Roy *et al.*,[17] is based on two loosely stabilized combs against two continuous-wave lasers with an "*a posteriori*" jitter correction. All the above approaches have been optimized for state-of-the-art capabilities, with acquisition times ranging from ~3 s to 24 h, spectral resolutions from 100 MHz to few GHz (depending on the single acquisition apodization window), optical bandwidths up to ~12 THz and signal-to-noise ratio (SNR) from 2500 to 316 000 in the spectral domain. However, they are all based on complicated setups, requiring two CW lasers for full jitter compensation, as well as custom post-processing electronic instrumentation, like fast Digital Signal Processor (DSP) or

[a]Author to whom correspondence should be addressed. Electronic mail: alessio.gambetta@polimi.it

 © 2014 AIP Publishing LLC

Field-Programmable Gate Array (FPGA) based acquisition boards[9,17] to record and handle the huge amount of data acquired. The final performances reached are well beyond the requirement of a simple spectrometer for "on-the-field" applications to gas sensing.

In this Letter, we demonstrate a simplified setup exploiting only a single free-running CW laser, in a transfer-oscillator configuration, for both real-time jitter compensation and absolute-referencing, without the need of custom electronics for data elaboration. This technique is demonstrated in the near-IR region, by exploiting a pair of free running femtosecond Er:fiber lasers and a fiber-coupled CW Extended-Cavity Diode Laser (ECDL) with emission wavelength at 1538 nm. Broadband dual-comb measurements over ~3.5 THz optical bandwidth are performed in a 1-s integration time, corresponding to a SNR enhancement of 29 dB compared to the single-shot acquisition. Signal recording and elaboration are done by a commercial 6.3 effective bits digital oscilloscope, without the use of digital acquisition boards.

The experimental setup is pictured in Fig. 1. Two free-running modelocked Er:fiber lasers (Menlo System M-Fiber and Menlo System M-Comb) at ~1.55 μm center wavelength and of ~250 MHz comb repetition frequency are employed. The main output (out1) of the first comb (comb1) passes through a 10-cm glass envelope sealed-cell filled with 50 millibars of C_2H_2 and is then launched by an objective into a standard telecom fiber. The fiber-coupled signal is combined by means of a 50/50 fiber coupler (OC1) with the second comb source (comb2) and the free-running interferogram trace is detected by a 100-MHz InGaAs photodetector (PD1). In order to achieve absolute frequency referencing as well as high SNR, a single-frequency (ν_{CW}) fiber-coupled ECDL is combined with both combs through a 50/50 fiber coupler (OC3), filtered by a narrow band-pass (1-nm bandwidth) fiber-coupled tunable optical filter, and sent to a 100-MHz photodetector (PD2). Two well distinct beat notes f_{b1} and f_{b2} between ν_{CW} and the nearest tooth of each comb are detected and their frequency spectrum is recorded by means of an electrical spectrum analyzer.

Fig. 2 depicts the referencing scheme. As shown in Fig. 2(b), each beat note is broadened by the frequency noise contribution (δ_m, δ_n) of the corresponding comb tooth and the frequency jitter (ε) of ν_{CW}. The instantaneous frequency difference Δf_b (extracted by amplifying and mixing f_{b1} with f_{b2}) encloses the information on the relative jitter $\Delta\delta = \delta_n - \delta_m$ between the corresponding comb modes ν_n and ν_m and it also univocally identifies the *kth* order of the discrete line of the RF spectrum (Fig. 2(c)). The jitter ε is cancelled in the mixing process as shown in the following expression:

$$\begin{aligned}\Delta f_b = f_{b2} - f_{b1} &= [(\nu_{CW} + \varepsilon) - (\nu_m + \delta_m)] \\ &-[(\nu_{CW} + \varepsilon) - (\nu_n + \delta_n)] = k\Delta f_r + \Delta\delta, \end{aligned} \quad (1)$$

where Δf_r is the difference between the repetition frequencies f_{r1} and f_{r2} of comb1 and comb2, respectively. Terms at f_{r1} are filtered out by a low-pass filter. To compensate for the jitter $\Delta\delta$, the RF spectrum of each interferogram is first rigidly shifted to higher frequencies by mixing with an offset signal f_{os} (using a low phase-noise synthesizer), then high pass filtered (HP0) to discard the lower-frequency replica and finally down-shifted again by mixing with the correction signal Δf_b, in order to cancel the jitter components correlated to $\Delta\delta$. Indeed, the compensation technique relies on the assumption that the relative jitter $\Delta\delta$ is constant over the whole optical bandwidth $\Delta\nu$. Such assumption is reasonable since the uncorrelated noise power spectral density is suppressed, owing to the small relative bandwidth $\Delta\nu/\nu_{CW}$ (less than 2%).[9] The corrected interferogram is acquired by a 6.3-effective-bits digital oscilloscope with real-time Fast-Fourier-Transform (FFT) capability, triggering on the interferogram peak. In the optical domain, each frequency f of the compensated RF spectrum corresponds to an absolute frequency ν given by the following equation:

$$\nu = (f - f_{os})\frac{f_{r1}}{\Delta f_r} + nf_{r1} + f_{01}, \quad (2)$$

where f_{01} is the offset frequency of comb1 and n is the mode order of comb1 frequency closer to ν_{CW}; n can unambiguously be determined once f_{01} and f_{r1} are known together with ν_{CW} and f_{b1}

$$n = \frac{\nu_{CW} - f_{b1} - f_{01}}{f_{r1}}. \quad (3)$$

The RF monitor port of the comb sources is exploited to retrieve the two pulse-train waveforms and to measure their

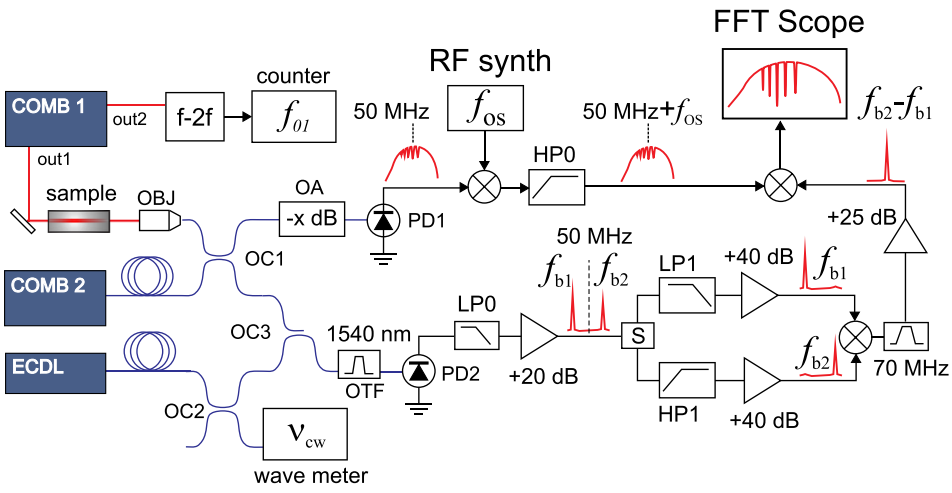

FIG. 1. Experimental setup. All optical components are fiber coupled. OBJ: fiber launcher, OC: optical coupler, OA: optical attenuator, OTF: tunable filter. PD: fast photodetector; LP, HP, BP: respectively, low-pass-, high-pass-, and band-pass filters. S: −3 dB power splitter.

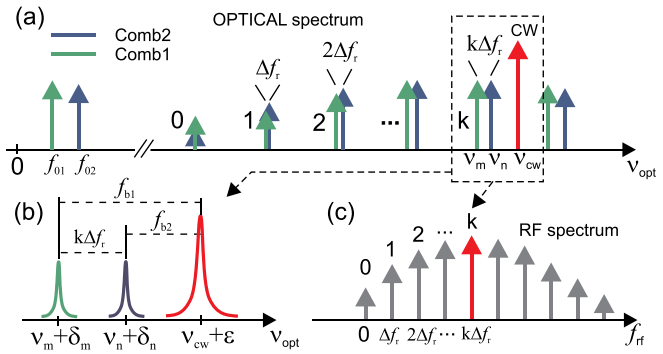

FIG. 2. (a) Frequency representation of the two comb sources overlapped with the CW source for absolute referencing. (b) Zoom on the CW laser and the two comb lines exploited for referencing and stabilization, each one broadened by the corresponding frequency jitter (respectively, ε, δ_n, δ_m), (c) dual comb RF discrete spectrum. The *kth* beat note corresponding to the ν_{CW} frequency position is evidenced in red.

repetition frequencies f_{r1} and f_{r2} by a dual-channel frequency counter with a gate time of 1 s. An f-2f interferometer, exploiting the second output (out2) of comb1, and a frequency counter are employed for the measurement of f_{01}, while a small portion (10%) of the power of the ECDL is sent to a wave-meter in order to measure ν_{CW} with an accuracy of ~50 MHz. Counter, RF synthesizer, and oscilloscope are all referenced to a GPS-disciplined low phase-noise rubidium oscillator.

Fig. 3(a) shows the f_{b1} and f_{b2} signals as detected by a fast photodiode. A SNR as high as 39 dB in a 100 kHz resolution-bandwidth (RBW) has been recorded with full-width at half maximum (FWHM) of about 300 kHz, mainly limited by the ECDL linewidth. The two beating signals should lie below and above 50 MHz, respectively, in

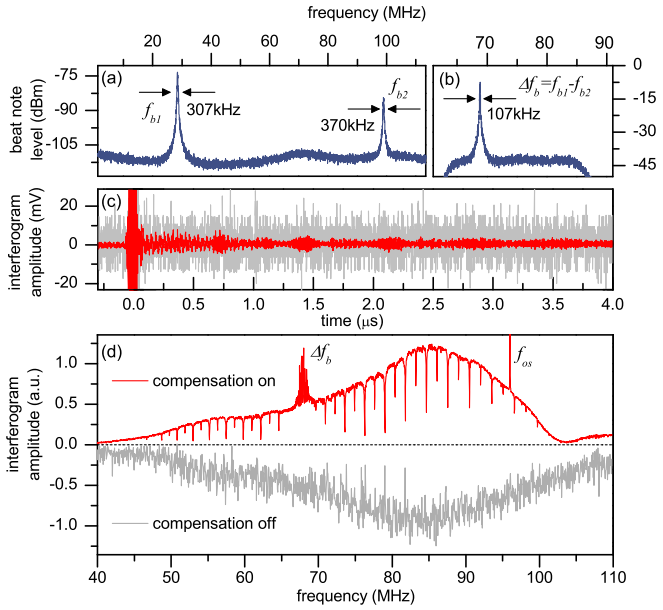

FIG. 3. (a) Beating signals f_{b1} and f_{b2} between ECDL and the two comb sources in a 100 kHz RBW. (b) Correction signal Δf_b obtained by mixing f_{b1} with f_{b2} (100 kHz RBW). (c) Free running single shot interferogram (gray) versus a 1000-times averaged jitter compensated interferogram (red). (d) Jitter-compensated spectrum obtained by FFT of the averaged interferogram (top red curve), compared to the free running single-shot spectrum (gray curve, inverted for clarity) acquired in a time window of 50 μs.

order to be frequency separated, amplified, and mixed, this is obtained by slow-locking the ECDL in order to compensate for ν_{CW} drifts. Fig. 3(b) displays the correction signal Δf_b characterized by a FWHM line-width of ~100 kHz (limited by the relative jitter of the two comb sources). A maximum SNR of 34 dB has been recorded for the correction signal. Fig. 3(c) compares two measurements corresponding, respectively, to a single shot free-running interferogram (gray) and a jitter-compensated interferogram 1000-times averaged over 1 s total acquisition time. The photodiode used for interferogram detection has a 2 mV noise floor and a ±500 mV saturation level. These circumstances, together with the low number of effective bits of the oscilloscope, make the very small absorption signal (only 7% of the interferogram peak) completely buried into quantization noise.

Fig. 3(d) compares the FFT spectra of the free-running (negative gray spectrum, flipped for clarity) and compensated interferograms (positive red spectrum). The artifacts at about 68 MHz and 96 MHz in the corrected spectrum are the residual Δf_b and f_{os} signals leaking through the RF mixer. The acquisition time of the single interferograms is 50 μs, with a Δf_r detuning of ~4.5 kHz. This value is a good compromise between the need of fast recording time and the highest possible bandwidth without aliasing of the optical frequencies in the RF spectrum. An instrumental-limited spectral resolution of ~1.1 GHz is achieved as a result of the chosen Δf_r detuning and the interferogram observation time window. The accuracy of the absolute optical axis is limited by the uncertainty on the measurement of Δf_r which, for a 1 s measurement, is of the order of 0.1 Hz (as retrieved from Allan-deviation measurements). The resulting overall accuracy is ~100 kHz, much lower than the instrumental resolution.

Despite the signal attenuation introduced by the analog mixer, the corrected spectrum presents a SNR of ~80 (measured in the frequency domain as the ratio between the strongest line and the corresponding root-mean-square (RMS) noise-floor level). An improvement of 29 dB as compared to the single-shot interferogram is obtained, making the absorption dips of the $\nu_1 + \nu_3$ acetylene overtone band clearly visible. Fig. 4(a) presents a comparison between the near-IR acetylene spectrum retrieved from HITRAN database (red dots) and the normalised, absolute frequency calibrated, corrected-spectrum (blue line). An empty cell is used for acquiring the reference spectrum for normalization. The RMS deviation of the peak absorption value is 7%, measured over the 36 most intense lines. For the same lines, a very good agreement is found between the measured center-peak frequency position and the center frequencies retrieved from HITRAN (and corrected for pressure-shift), with an overall standard deviation of ~98 MHz, as shown in Fig. 4(b). This value is comparable to the accuracy of the center frequency of the Voigt-profile fit, which is limited by the SNR and the number of experimental points covering the absorption line. The 3.3 GHz spectral width of the measured absorption lines is larger than the value of 1.6 GHz obtained by convolving the theoretical linewidth with the spectral response of the observation time window: this discrepancy is ascribed to time-fluctuations of the oscilloscope trigger events, resulting in a residual jitter of the RF comb spectrum. The actual

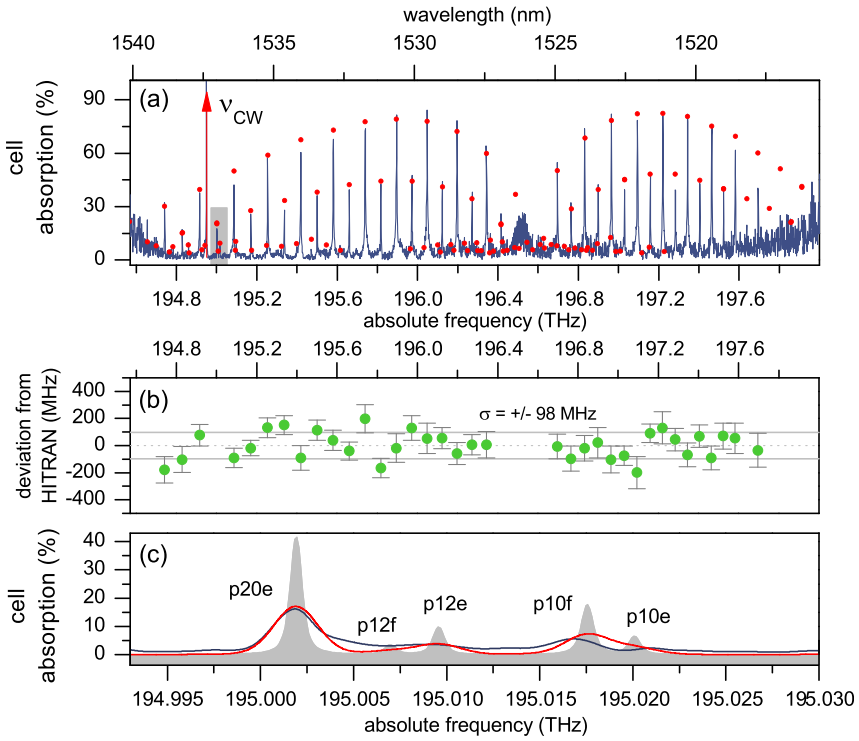

FIG. 4. (a) Absorption-spectrum of the C_2H_2-filled cell, plotted versus the absolute calibrated optical frequency (blue line). Red dots: absorption peak-intensities calculated using HITRAN database for a 10 cm long, 50 millibars C_2H_2 filled cell, and a 3 GHz instrumental resolution. A zoom of the square shaded area is plotted in panel (c). (b) Deviation from HITRAN database of the center of the fitted peaks (green dots) and uncertainties of the fitted peak center (gray error bars). (c) Zoom of the dual-comb spectrum around 195 THz (blue) compared with an HITRAN-based simulation accounting for broadening effects due to residual jitter and instrumental spectral response (red). Theoretical line shapes are represented by the gray-shaded area for comparison.

calculated resolution is of 2.6 GHz. Fig. 4(c) compares a small frequency portion of the dual comb spectrum around 195 THz (blue line) with the theoretical absorption of the gas sample cell (gray-shaded area) and the simulated absorption taking into account the spectral broadening due to both residual comb jitter and FFT window response (red line). It is worth noting that, although with much greater uncertainty on the peak position due to the poor SNR, features with line strengths of the order of 10^{-22} cm^{-1} mol^{-1} cm^2, like the p12e and p10f absorption peaks, can still be distinguished in the dual-comb spectrum. The NEA calculated over the 36 most intense lines[8,9] is 1.9×10^{-4} cm^{-1} Hz$^{-0.5}$, equivalent to a detection limit of ~60 ppm of acetylene by volume. This value is limited by the very short absorption-path length of the 10 cm sample cell used. Values of 6.3×10^{-7} cm^{-1} Hz$^{-0.5}$ (~200 ppb of C_2H_2) and 2.6×10^{-8} cm^{-1} Hz$^{-0.5}$ (~7 ppb of C_2H_2) could be reached, respectively, by using a 30 m optical-path multi-pass cell or a ~1200 Finesse cavity.

In conclusion, a simple technique for real-time jitter compensation and absolute-referencing of dual-comb measurements is demonstrated. This technique, employing a single CW laser, has been applied to a near-IR dual-comb setup based on a pair of mode locked Er:fiber lasers. By probing a 10 cm cell filled with 50 millibars of C_2H_2, a broadband optical spectrum of ~3.5 THz span, with 2.6 GHz spectral resolution, has been recorded in a 1 s integration time. Compared to the single-shot measurement, a SNR increase of 29 dB has been achieved corresponding to a 1.9×10^{-4} cm^{-1} Hz$^{-0.5}$ NEA. This value could be further scaled down by a factor of 10^3 and 10^4, respectively, by using a multi-pass cell or a resonant cavity. This approach can be as well used with dual comb spectrometers in the mid-IR region, taking advantage of the more intense molecular line-strengths of the fingerprint region for a further enhancement of the sensitivity.

The authors wish to thank the Italian Ministry of University and Research (FIRB Project No. RBFR1006TZ and Extreme Light Infrastructure-Italy ELI-Italy) for financial support.

[1]T. Udem, R. Holzwarth, and T. W. Hänsch, Nature **416**, 233 (2002).
[2]S. A. Diddams, J. Opt. Soc. Am. B **27**, B51–B62 (2010).
[3]A. Gambetta, D. Gatti, A. Castrillo, G. Galzerano, P. Laporta, L. Gianfrani, and M. Marangoni, Appl. Phys. Lett **99**, 251107 (2011).
[4]M. J. Thorpe, K. D. Moll, R. J. Jones, B. Safdi, and J. Ye, Science **311**, 1595–1599 (2006).
[5]S. A. Diddams, L. Hollberg, and V. Mbele, Nature **445**, 627–630 (2007).
[6]J. Mandon, G. Guelachvili, and N. Picqué, Nat. Photonics **3**, 99–102 (2009).
[7]A. Cingöz, D. C. Yost, T. K. Allison, A. Ruehl, M. E. Fermann, I. Hartl, and J. Ye, Nature **482**, 68–71 (2012).
[8]F. Adler, P. Masłowski, A. Foltynowicz, K. Cossel, T. Briles, I. Hartl, and J. Ye, Opt. Express **18**, 21861–21872 (2010).
[9]I. Coddington, W. C. Swann, and N. R. Newbury, Phys. Rev. A **82**, 043817 (2010).
[10]B. Bernhardt, A. Ozawa, P. Jacquet, M. Jacquey, Y. Kobayashi, Th. Udem, R. Holzwarth, G. Guelachvili, T. W. Hänsch, and N. Picqué, Nat. Photonics **4**, 55–57 (2010).
[11]S. Schiller, Opt. Lett. **27**, 766 (2002).
[12]F. Keilmann, C. Gohle, and R. Holzwarth, Opt. Lett. **29**, 1542 (2004).
[13]F. Zhu, T. Mohamed, J. Strohaber, A. A. Kolomenskii, Th. Udem, and H. A. Schuessler, Appl. Phys. Lett **102**, 121116 (2013).
[14]B. Bernhardt, E. Sorokin, P. Jacquet, R. Thon, T. Becker, I. T. Sorokina, N. Picqué, and T. W. Hänsch, Appl. Phys. B **100**, 3–8 (2010).
[15]T. Ideguchi, A. Poisson, G. Guelachvili, T. W. Hänsch, and N. Picqué, Opt. Lett. **37**, 4847 (2012).
[16]T. Ideguchi, A. Poisson, G. Guelachvili, N. Picqué, and T. W. Hänsch, Nat. Commun. **5**, 3375 (2014).
[17]J. Roy, J.-D. Deschênes, S. Potvin, and J. Genest, Opt. Express **20**, 21932 (2012).